doi:10.3772/j.issn.1006-6748.2019.03.010

Structural optimization and stability analysis of the ducted fan unmanned aerial vehicles①

Fu Weijie(符伟杰)[*,**], Chen Cheng②[*,**], Li Wenchao[****], Zhang Yonghong[***], Chu Zefan[*,**]
([*] Nanjing Automation Institute of Water Conservancy and Hydrology, Nanjing 210012, P. R. China)
([**] Hydrology and Water Resources Engineering Research Center for Monitoring, Nanjing 210012, P. R. China)
([***] Nanjing University of Information Science and Technology, Nanjing 210044, P. R. China)
([****] Agricultural Rural and Hydrological Bureau of Subei Mongolian Autonomous County, Jiuquan 736300, P. R. China)

Abstract

This article investigates the improvement of dynamics stability of the ducted fan unmanned aerial vehicles(UAVs) by optimizing its mechanical-structure parameters. The instability phenomenon of the ducted fan unmanned aerial vehicles takes place frequently that easily leads to vibration and even out of control, due to complicated airflow. The dynamics equations mirror its dynamics characteristics, which is primarily influenced by the mechanical-structure parameters of the whole system. Based on this, the optimization of mechanical-structure parameters will improve the dynamics stability of the whole system. Therefore, this paper uses the concept of Lyapunov exponents to build the quantification relationship between system's mechanical-structure parameters and its motion stability to enhance its stability. The simulation experimental results indicate that compared with the direct Lyapunov method, the most important advantage of the proposed method is its constructivity, so it is an effective tool for analysis of the motion stability of other non-linear systems such as robots.

Key words: Lyapunov exponents (LEs), ducted fan unmanned aerial vehicles(UAVs), mechanical-structure parameters, dynamics stability

0 Introduction

With their small size, compact layout and strong maneuverability, the ducted fan unmanned aerial vehicles (ducted fan UAVs) are regarded as great candidates to perform bomb attack, goods delivery and other flight tasks[1,2]. However, owing to the atmospheric disturbances, gyroscopic effects and other unpredictable factors, the ducted fan UAVs are easily subject to shaking and other dynamics stability phenomena[3-5]. Therefore, it is specifically important to investigate its variable-structure parameters to enhance the dynamics stability of the whole system.

Currently, there are two major methods in the control theory. The first is to directly solve dynamics equations. The second is represented by Lyapunov who published the famous Ph. D dissertation on general movement stability problems, which marked a new epoch in motion stability studies. The extreme difficulty is to apply the Lyapunov stability analysis that will find a Lyapunov function. Furthermore, there is no general rule to get a Lyapunov function for nonlinear system. As a result, the stability of many complex nonlinear dynamical systems cannot be researched. On the other hand, an alternative method is used to analyze the stability of the nonlinear dynamical system, which is the concept of Lyapunov exponents (LEs)[6]. LEs can be described as the average exponential rates of divergence or convergence of orbits nearby in the state space, which can imply system's stability. When the numerical value of LE, the system is stable or it is chaotic[7,8].

Calculation of LEs using a dynamics equation has been well known[9]. Besides, many complex nonlinear systems have been used for stability using the LEs. For instance, Sadri et al[10], Yang et al[11], Wu et al[12] conducted the stability analysis of biped standing using the concept of LEs. Omar et al[13] improved the robustness using Lyapunov stability. The optimization of mechanical-structure parameters is used to investigate a series of accomplishments to improve the stability of

① Supported by the National Natural Science Foundation of China (No. 51575283) and Central Public Welfare Basic Scientific Research Institute Special Funds (No. Y919008).
② To whom correspondence should be addressed. E-mail: chencheng_nuist@sina.com
Received on Sep. 9, 2018

whole system[14,15]. Therefore, it is justified to use LEs as the quantitative stability of the ducted fan UAVs to increase dynamics stability via the optimization of the mechanical-structure parameters.

1 Methodology

1.1 Modeling

Before constructing a dynamics equation of the system, two reference frames will be defined, the inertial reference frame and the body fixed reference frame. A ground frame could be closed to the inertial reference frame for local flight to derive the equations of the ducted fan UAVs motion. The ground reference frame has its origin fixed to the ground, generally at the starting point, and the three axes constitute NED (North-East-Down) coordinate[16]. The body fixed reference frame has its origin fixed in the center of gravity of the ducted fan UAVs. The body fixed reference frame is shown in Fig. 1. The ϕ, θ and ψ are the attitude angles, x, y and z are linear displacement, p, q and r are angular velocities, u, v and w are linear velocities about x, y and z axis, respectively. However, some assumptions are regarded as follows: 1) The body is considered as rigid body; 2) Ignoring air friction and other tiny resistance.

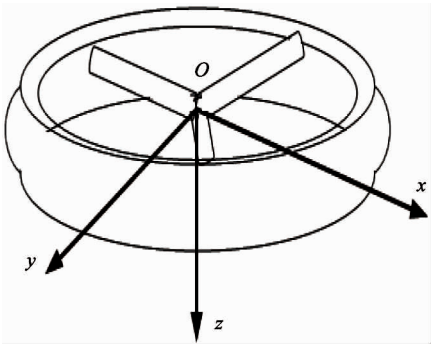

Fig. 1 Simplified vehicle model of the 6-DOF

The dynamics and kinematics equation can be written as the Poincaré's equations[17]:

$$\dot{\boldsymbol{q}} = \boldsymbol{V}(\boldsymbol{q})\boldsymbol{p} \tag{1}$$

$$\boldsymbol{M}(\boldsymbol{q})\dot{\boldsymbol{p}} + \boldsymbol{C}(\boldsymbol{q}, \boldsymbol{p})\boldsymbol{p} + \boldsymbol{F}(\boldsymbol{p}, \boldsymbol{q}, \boldsymbol{u}) = 0 \tag{2}$$

where $\boldsymbol{q} = (\phi, \theta, \psi, x, y, z)^{\mathrm{T}}$, $\boldsymbol{p} = (p, q, r, u, v, w)^{\mathrm{T}}$, $\boldsymbol{V}(\boldsymbol{q})$, $\boldsymbol{M}(\boldsymbol{q})$, $\boldsymbol{C}(\boldsymbol{q}, \boldsymbol{p})$ and $\boldsymbol{F}(\boldsymbol{p}, \boldsymbol{q}, \boldsymbol{u})$ are the kinematic matrix, inertial matrix, gyroscopic matrix and force function, respectively. The force function contains the aerodynamic, gravitational force, momentum and so on.

$$\boldsymbol{V}(\boldsymbol{q}) = \begin{bmatrix} 1 & 0 & 0 & 0 & 0 & 0 \\ S_\theta T_\theta & C_\phi & S_\phi C_\theta^{-1} & 0 & 0 & 0 \\ C_\phi T_\theta & -S_\psi & C_\psi C_\theta^{-1} & 0 & 0 & 0 \\ 0 & 0 & 0 & C_\theta C_\psi & C_\theta S_\psi & -S_\theta \\ 0 & 0 & 0 & S_\phi S_\theta C_\psi - C_\phi S_\psi & S_\phi S_\theta S_\psi + C_\phi S_\psi & S_\phi C_\theta \\ 0 & 0 & 0 & C_\phi S_\theta C_\psi + S_\phi S_\psi & C_\phi S_\theta S_\psi - S_\phi C_\psi & C_\phi C_\theta \end{bmatrix} \boldsymbol{F}(\boldsymbol{p}, \boldsymbol{q}, \boldsymbol{u}) = \begin{bmatrix} -\sum M_x \\ -\sum M_y \\ -\sum M_z \\ -\sum F_x + gmS_\theta \\ -\sum F_y - gmC_\theta S_\psi \\ -\sum F_z - gmC_\theta S_\psi \end{bmatrix}$$

$$\boldsymbol{C}(\boldsymbol{q}, \boldsymbol{p}) = \begin{bmatrix} 0 & -I_y r & I_z q & 0 & -mw & mv \\ I_x r & 0 & -I_z p & mw & 0 & -mu \\ -I_x q & I_y p & 0 & -mv & mu & 0 \\ 0 & 0 & 0 & 0 & -mr & mq \\ 0 & 0 & 0 & mr & 0 & -mp \\ 0 & 0 & 0 & -mq & mp & 0 \end{bmatrix} \quad \boldsymbol{M}(\boldsymbol{q}) = \begin{bmatrix} I_x & 0 & 0 & 0 & 0 & 0 \\ 0 & I_y & 0 & 0 & 0 & 0 \\ 0 & 0 & I_z & 0 & 0 & 0 \\ 0 & 0 & 0 & m & 0 & 0 \\ 0 & 0 & 0 & 0 & m & 0 \\ 0 & 0 & 0 & 0 & 0 & m \end{bmatrix}$$

where m is system mass, g is gravity acceleration, I_x, I_y, and I_z are the moment of inertia. $\sum M_x$, $\sum M_y$, $\sum M_z$ and $\sum F_x$, $\sum F_y$, $\sum F_z$ are momentums and forces acting on the body x, y and z axes, respectively. Moreover, $C_\theta = \cos(\theta)$, $C_\theta^{-1} = \sec(\theta)$, $T_\theta = \tan(\theta)$, $C_\psi = \cos(\psi)$, $S_\phi = \sin(\phi)$, $S_\psi = \sin(\psi)$, $C_\phi = \cos(\phi)$, $S_\theta = \sin(\theta)$.

Meanwhile, the proportional-derivative (PD) controller will be used to control the ducted fan (UAVs) at the hovering state. For the PD controller, the torque at each joint is:

$$T_i = k_{pi}(\theta_{di} - \theta_i) + k_{di}(\dot{\theta}_{di} - \dot{\theta}_i),\ i = 1,2 \tag{3}$$

where θ_{di} is the desired position, k_{pi} and k_{di} are the proportional and derivative gains.

There are several forces and momentums, the gravity, lift, control surface and fuselage acting on the vehicle, respectively [18-20].

Gravity

$$\begin{aligned} F_{Gx} &= -gm\sin(\theta) \\ F_{Gy} &= -gm\cos(\theta)\cos(\psi) \\ F_{Gz} &= gm\cos(\theta)\sin(\psi) \end{aligned} \tag{4}$$

$$M_{Gx} = M_{Gy} = M_{Gz} = 0 \tag{5}$$

Airfoil

The lift of airfoil can be generated as

$$F_{Bx} = F_{By} = 0$$

$$\begin{aligned} F_{Bz} &= -T \\ M_{Bx} &= M_{By} = 0, \\ M_{Bz} &= -M_e \end{aligned} \tag{6}$$

$$T = \frac{1}{4}N_b(v_b - v_i)\omega_r r^2 \rho a_0 b c_r,$$

$$v_b = v_i + \frac{2}{3}\omega_r r\left(\frac{3}{4}K_{twist}\right),$$

$$M_e = N_b\int_0^r \frac{1}{2}\rho\omega_r r^3 C_D \mathrm{d}r$$

where v_i represents the induced velocity via the rotor, a_o stands for rotor lift curve coefficient, b denotes the number of the rotor blades, c_r, ρ, N_b, r, ω_r, k_{twist} and C_D are the rotor blade chord, air density, number of airfoil, radius of the rotor, angular velocity, twist of the blades, and drag coefficients of the vehicle, respectively.

Control surface

The forces and momentums are applied to the vehicle via the control surface, which can be written as

$$\begin{aligned} F_{Cx} &= 2\,\frac{1}{2}\rho v_i^2 S_t C_l(\delta_1)\sin(\delta_1) \\ F_{Cy} &= 2\,\frac{1}{2}\rho v_i^2 S_t C_l(\delta_2)\sin(\delta_2) \\ F_{Cz} &= 2\,\frac{1}{2}\rho v_i^2 S_t C_l(\delta_1)\sin(\delta_1) \\ &\quad + 2\,\frac{1}{2}\rho v_i^2 S_t C_l(\delta_2)\sin(\delta_2) \\ &\quad + 4\,\frac{1}{2}\rho v_i^2 S_t C_l(\delta_3)\sin(\delta_3) \end{aligned} \tag{8}$$

$$\begin{aligned} M_{Cx} &= 2\,\frac{1}{2}\rho v_i^2 S_t C_l(\delta_1) L_1 \\ M_{Cy} &= 2\,\frac{1}{2}\rho v_i^2 S_t C_l(\delta_2) L_2 \\ M_{Cz} &= 4\,\frac{1}{2}\rho v_i^2 S_t C_l(\delta_3) L_3 \end{aligned} \tag{9}$$

where δ_1, δ_2 and δ_3 are control vane bias, L_1, L_2 and L_3 are the arms of forces, respectively.

Fuselage

As in the hovering, $u=0$, $v=0$, $w=0$. Owing to the fuselage aerodynamic drag, the forces and the momentums can be generated as

$$\begin{aligned} F_{Dx} &= -\frac{1}{2}\rho C_x u^2 S_x \\ F_{Dy} &= \frac{1}{2}\rho C_y v^2 S_y \\ F_{Dz} &= \frac{1}{2}\rho C_z w^2 S_z \end{aligned} \tag{10}$$

$$M_{Dx} = M_{Dy} = M_{Dz} = 0 \tag{11}$$

where C_x, C_y and C_z are the coefficient of lift; S_x, S_y and S_z are vehicle platform area.

Eqs(4) – (11) can be expressed as

$$\begin{aligned} \sum F_x &= F_{Gx} + F_{Bx} + F_{Cx} + F_{Dx} \\ \sum F_y &= F_{Gy} + F_{By} + F_{Cy} + F_{Dy} \\ \sum F_z &= F_{Gz} + F_{Bz} + F_{Cz} + F_{Dz} \end{aligned} \tag{12}$$

$$\begin{aligned} \sum M_x &= M_{Gx} + M_{Bx} + M_{Cx} + M_{Dx} \\ \sum M_y &= M_{Gy} + M_{By} + M_{Cy} + M_{Dy} \\ \sum M_z &= M_{Gz} + M_{Bz} + M_{Cz} + M_{Dz} \end{aligned} \tag{13}$$

Combining the kinematics Eq. (1), dynamics Eq. (2) with Eq. (12) and Eq. (13), the state equations can be obtained:

$$\dot{q} = \begin{bmatrix} p + qS_\phi T_\theta + rC_\phi T_\theta \\ qC_\phi - rS_\phi \\ qS_\phi C_\theta^{-1} + rC_\phi C_\theta^{-1} \\ uC_\theta C_\psi + v(S_\theta S_\phi C_\psi - C_\phi S_\psi) + w(S_\theta C_\phi C_\psi + S_\phi S_\psi) \\ u(C_\theta S_\psi) + v(S_\theta S_\phi S_\psi + C_\phi C_\psi) + w(C_\phi S_\theta S_\psi - S_\phi C_\psi) \\ -uS_\theta + vS_\phi C_\theta + wC_\phi C_\theta \end{bmatrix} \tag{14}$$

$$\dot{p} = \begin{bmatrix} (\sum M_x - qr(I_z - I_y))/I_x \\ (\sum M_y - rp(I_x - I_z))/I_y \\ (\sum M_z - pq(I_y - I_x))/I_z \\ -(qw - rv) + \frac{1}{m}\sum F_x \\ -(ru - pw) + \frac{1}{m}\sum F_y \\ -(pv - qu) + \frac{1}{m}\sum F_z \end{bmatrix} \tag{15}$$

1.2 Numerical calculation of Lyapunov exponents (LEs)

When Eq. (14) is combined with Eq. (15), the nonlinear equations of the ducted fan UAVs can be written as

$$\dot{X} = f(X) \tag{16}$$

where $X = [\boldsymbol{q}, \boldsymbol{p}]^{\mathrm{T}} = (\phi, \theta, \psi, x, y, z, p, q, r, u, v, w)^{\mathrm{T}}$ is state variable.

The calculation of LEs based on dynamics equation can be written as

$$\lambda = \lim_{n\to\infty}\frac{1}{n}\sum_{i=0}^{n-1}\ln\left|\frac{\mathrm{d}f(X)}{\mathrm{d}X}\right|_{X_i} \tag{17}$$

To calculate LEs spectrum $\lambda_1, \lambda_2, \cdots, \lambda_6$, let time $T=0.01$ s and iterations $k=100$. With regard to

k^{th} iteration ($k=1, 2, \cdots, k$), the initial conditions of variation Eq. (16) is set to $\{v_1^{(k-1)}, v_2^{(k-1)}, \cdots, v_6^{(k-1)}\}$. The $\{v_1^{(k-1)}, v_2^{(k-1)}, \cdots, v_6^{(k-1)}\}$ is translated into $\{w_1^{(k-1)}, w_2^{(k-1)}, \cdots, w_6^{(k-1)}\}$ after Ts integration. Then, the $\{w_1^{(k-1)}, w_2^{(k-1)}, \cdots, w_6^{(k-1)}\}$ is converted into $\{u_1^{(k-1)}, u_2^{(k-1)}, \cdots, u_6^{(k-1)}\}$ through the Gram-Schm-orthogonal, the ultimate vector value is $\{u_1^k, u_2^k, \cdots, u_6^k\}$. Repeat this process and k is chosen large enough[5,21].

LEs theory will be used to establish the quantitative relationship between dynamics stability of the whole system and mechanical-structure parameters shown in Fig. 2.

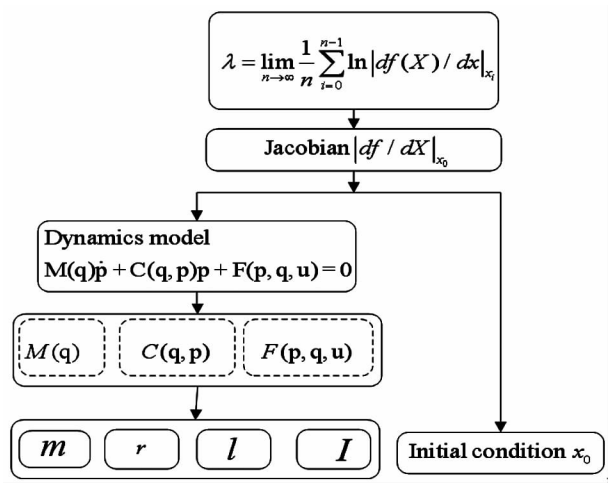

Fig. 2 Between Lyapunov Exponents and structural parameters

2 Simulation results

2.1 Parameter identification

To obtain numerical dynamics polynomial of the ducted fan UAVs, m, g, I_x, I_y, I_z, a_o, b N_b and so on need to be acquired. Here, mechanical-structure parameters of the vehicle are listed in Table 1. In simulation analysis, mathematica in the PC environment is used to obtain dynamics models for the ducted fan (UAVs), when the system locates in take-off, landing and hovering stage, respectively.

2.2 Take off stage

With the propeller speed increasing slowly, when the total tensile force in the z axis is larger than its gravity, the ducted fan UAV displays take-off state in NED (North-East-Down) coordinate. It can be seen that the attitude of curve $y(t)$, $z(t)$ display raise and $x(t)$ displays declining, which is shown in Fig. 3.

Table 1 The value of mechanical-structure parameters of the system

Parameters	Value
m	15.5 kg
g	9.8 m/s^2
I_x, I_y, I_z	2.374 kg · m^2, 2.374 kg · m^2, 0.8437 kg · m^2
a_o	5.9
b	5
N_b	1
r	0.4 m
ω_r	500 rpm
v_i	20 m/s
C_x, C_y, C_z	0.5, 0.5, 0.1
L_1, L_2, L_3	0.26, 0.26, 0.275 m
k_{wist}	0.2618
C_r	0.025 m
A	0.5024 m^2
C_l	0.12
C_D	0.5
ρ	1.29 kg/m^2

2.3 Landing stage

When the speed of rotor of the vehicle decreases, landing state emerges, as shown in Fig. 4. The curve $x(t)$, $y(t)$ and $z(t)$ will be decreasing.

It can be drawn that the convergence speed of Lyapunov exponents spectrum $\lambda(\phi)$, $\lambda(\theta)$, $\lambda(\psi)$, $\lambda(x)$, $\lambda(y)$ and $\lambda(z)$ to zero or negative value at take-off state in Fig. 5. Meanwhile, Fig. 6 also shows the identical results. The simulation results reveal that the convergence speed of LEs spectrum at take-off stage approaching to 0 or negative values is faster than that of landing stage according to Figs 5 and 6. Therefore, the results also indicate that the dynamics stability of system at take-off state is better than that at landing. Practically, the ducted fan UAVs have much more better take-off state and it is hard to make a smooth landing. This phenomenon can be used to interpret that aircraft is more possible to crash compared with landing state.

For the parametric diversity, based on the structural stability analysis, significant insights into the effects of the radius of rotor on the system have been studied. Other mechanical-structure parameters are not changed and the value of the rotor radius r is enhanced to 0.6 m (the modified value r is equivalent to 0.6 m, and the original value is equivalent to 0.4 m). Curve of attitude and the spectrum of LEs are shown in Figs7 and 8 via the optimization of structural parameter r, respectively. Seeing from the Fig. 7, it has been revealed that the attitude of the curve $x(t)$, $y(t)$ and $z(t)$ will

be greatly decreased compared with Fig. 4. Compared with Fig. 6 and Fig. 8, it can be discovered that the value of LEs spectrum at the modified landing state to negative values are larger than that during the original landing state. Besides, the arm of force $L3$ is changed with, $L3 = 0.55$ m, other parameters are kept unchanged. The system spectrum of Lyapunov exponents is shown in Fig. 9. As seen from Fig. 9, when the value of $L3$ enhances from $L3 = 0.275$ m to $L3 = 0.55$ m, the convergence speed of Lyapunov exponents spectrum to negative is faster compared with $L3 = 0.255$ m, that is, system stability can be improved by changing the rotor radius $L3$. Therefore, changing mechanical-structure parameters can be used to improve its dynamics stability.

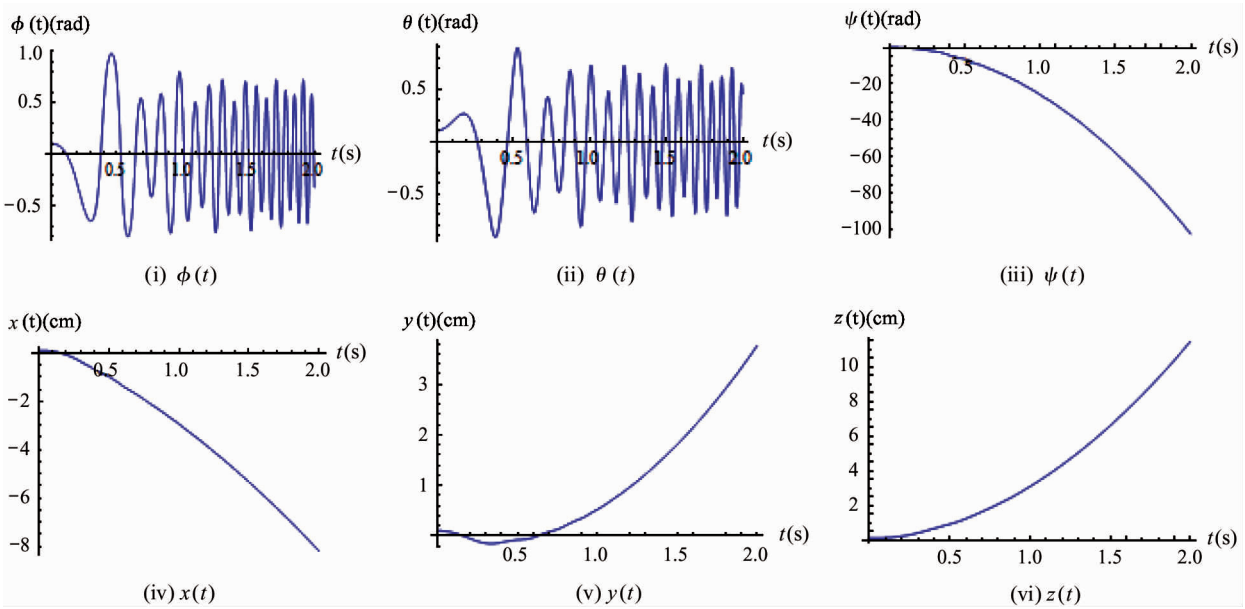

Fig. 3 The curve of attitude at take-off state

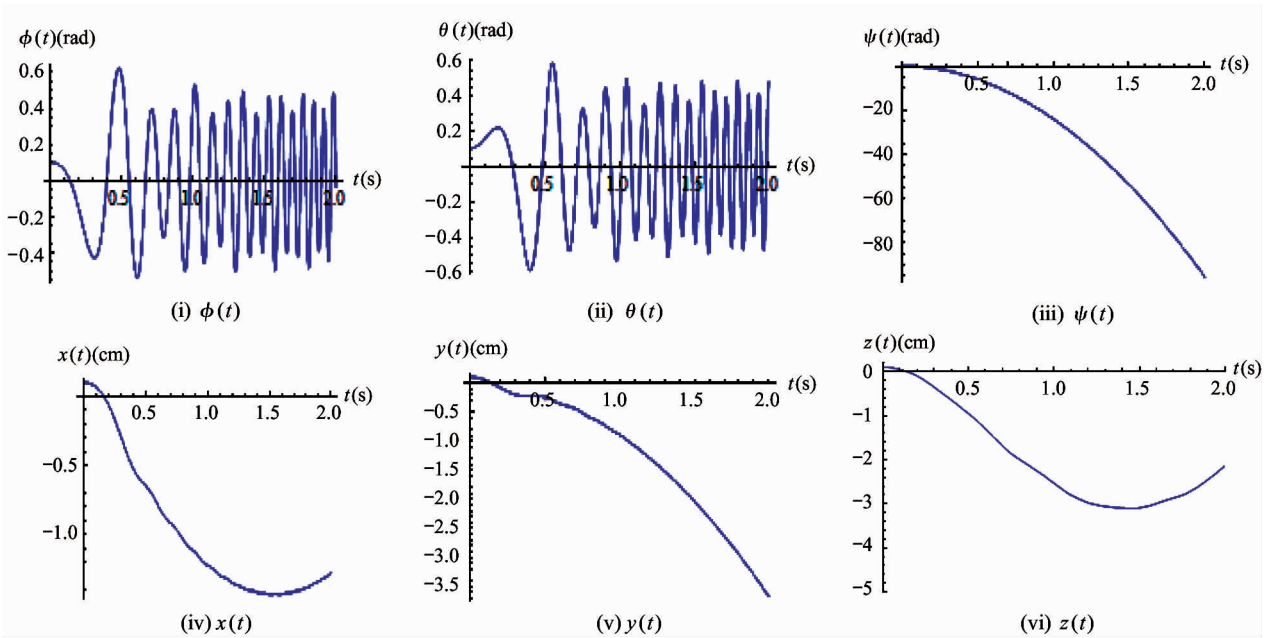

Fig. 4 The curve of attitude at landing state

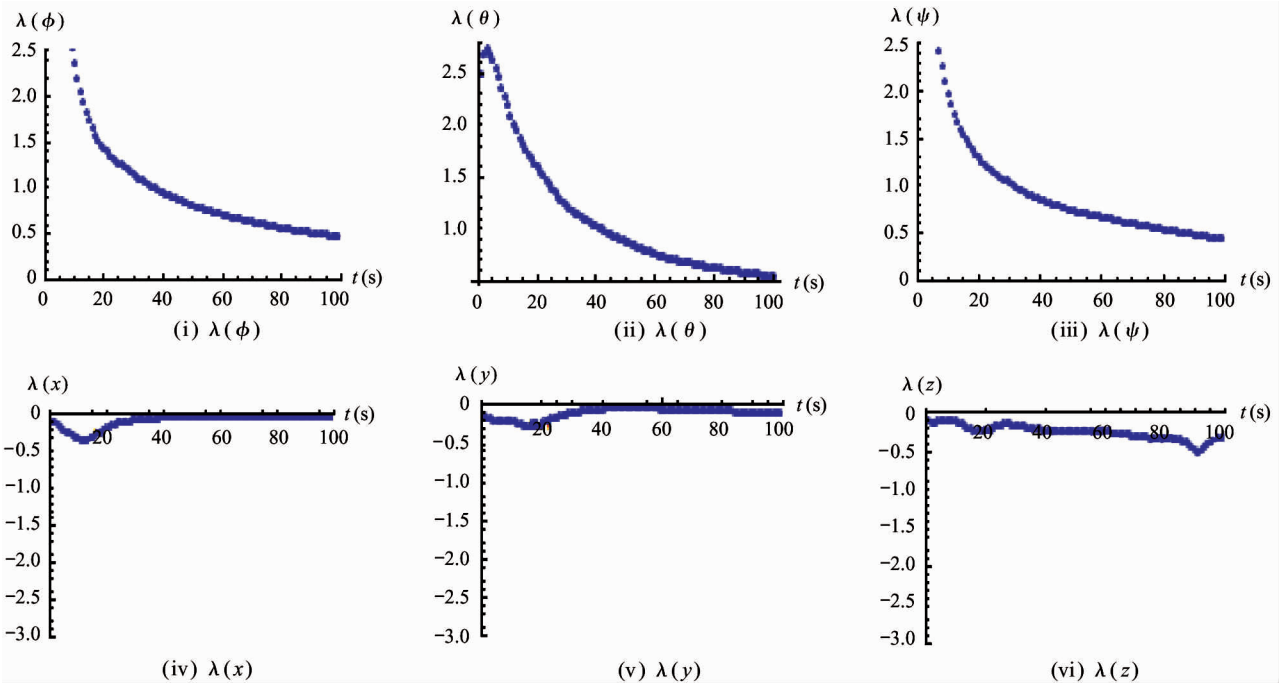

Fig. 5 Lyapunov exponents spectrum during take-off state

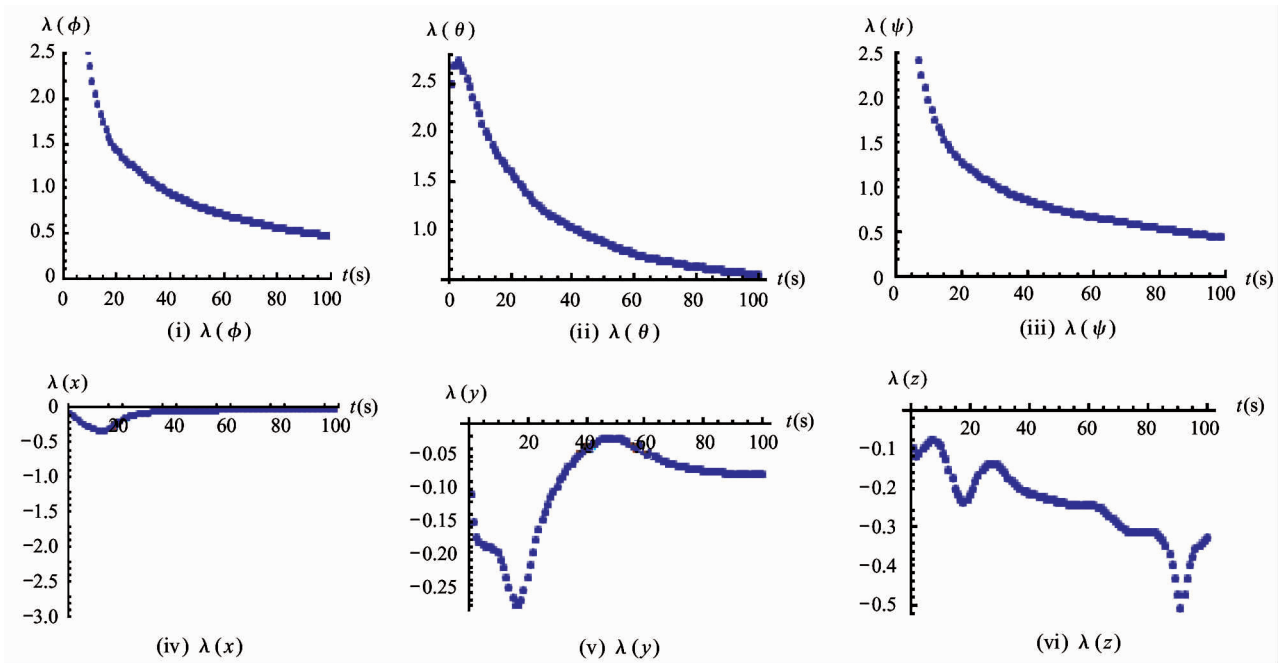

Fig. 6 Lyapunov exponents spectrum during landing stage

2.4 Hovering stage

In this section, by setting $\theta_{d1} = \phi = 0.7\sin(2\phi)$, $\theta_{d2} = \theta = 0.7\sin(2\theta)$ and $\theta_{d3} = \psi = 0.7\sin(2\psi)$, and the controller gains were chosen as $k_{p1} = 170$ N/rad, $k_{d1} = 40$ NS/rad; $k_{p2} = 90$ N/rad, $k_{d2} = 10$ NS/rad and $k_{p3} = 110$ N/rad, $k_{d3} = 10$ NS/rad in the simulations. Fig. 10 (i), (ii) and (iii) reveal that $\lambda(\phi)$, $\lambda(\theta)$ and $\lambda(\psi)$ take about 40 s converging to negative values, indicating the system has been successfully driven to the steady state. Therefore, for the controller gain chosen is reasonable, Fig. 10 (i), (ii) and (iii) show that the attitude of the curve $\phi(t)$, $\theta(t)$ and $\psi(t)$ maintains standard trajectory (the angle is approximately equal to 0) after around 3 s (the dash lines are the desired trajectories and the solid lines are the actual trajectories).

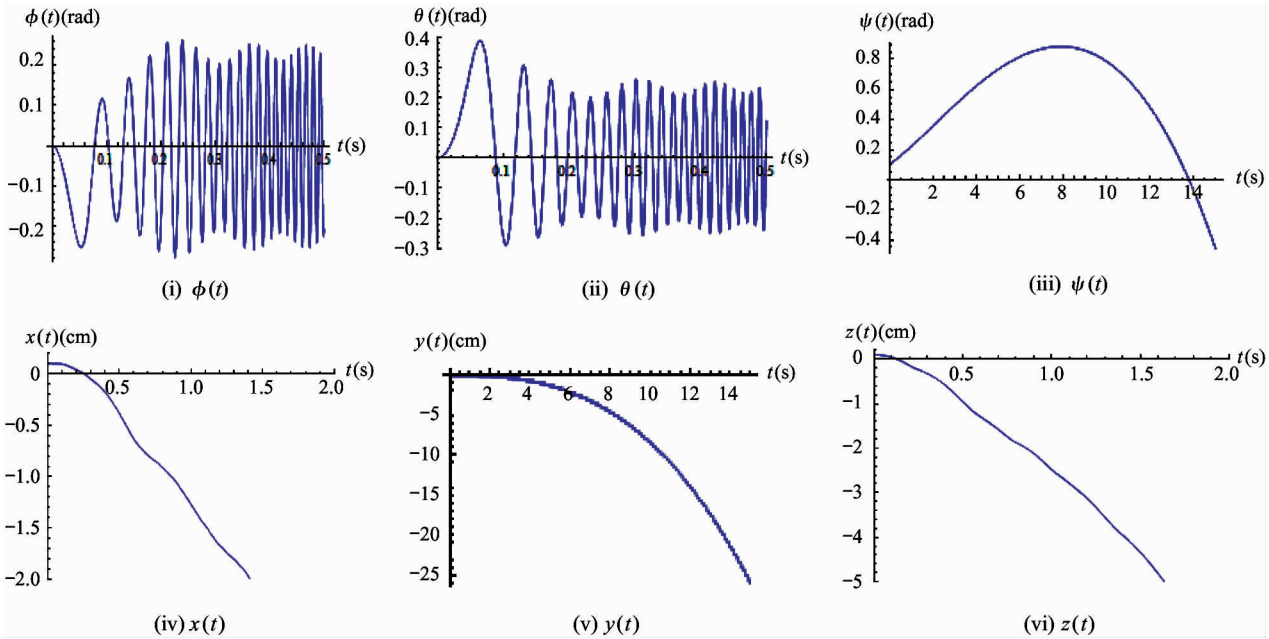

Fig. 7 Modified curve of attitude at landing state

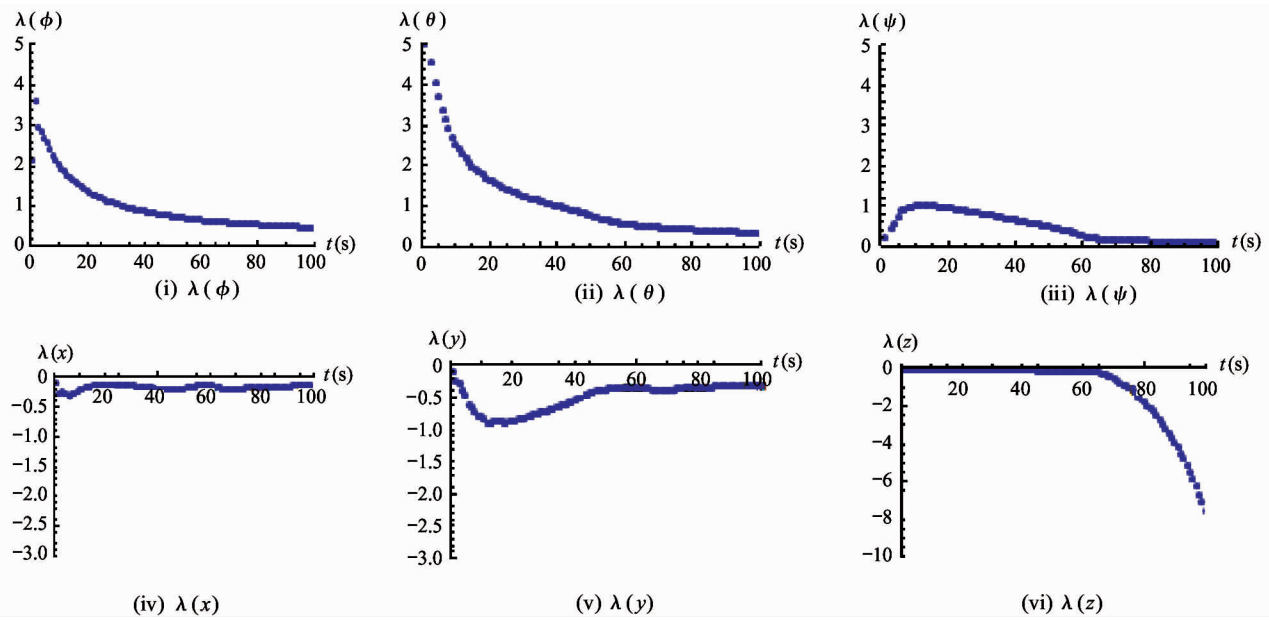

Fig. 8 Modified Lyapunov exponents spectrum during landing stage

Meanwhile, let $\theta_{d4} = x = 1.7\sin(2x)$, $\theta_{d5} = y = 1.7\sin(2y)$ and $\theta_{d6} = z = 1.7\sin(2z)$; also, the controller gains are selected as $k_{p4} = 1$ N/rad, $k_{d4} = 300$ NS/rad; $k_{p5} = 2$ N/rad, $k_{d5} = 350$ NS/rad and $k_{p6} = 2$ N/rad, $k_{d6} = 250$ NS/rad, it has been shown that all of LEs are negative values, suggesting the system is stable, as shown in Fig. 10(iv), (v) and (vi). Fig. 10(iv), (v) and (vi) also show that the linear displacement can successfully keep the horizontal trajectory (the linear displacement is approximately equal to 0). Based on the analysis, it is found that the LEs spectrum is taken to converge to 0 or negative values, suggesting that the system has been successfully driven to the steady state.

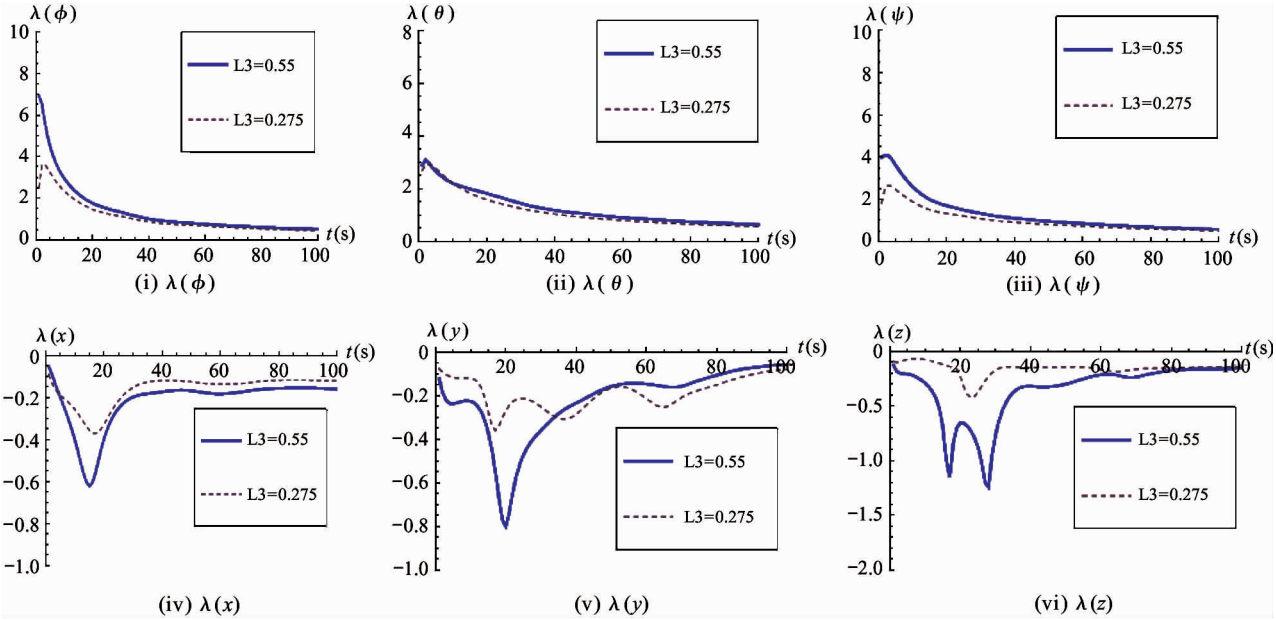

Fig. 9 Lyapunov exponents spectrum during landing stage ($L3 = 0.55$ and $L3 = 0.275$)

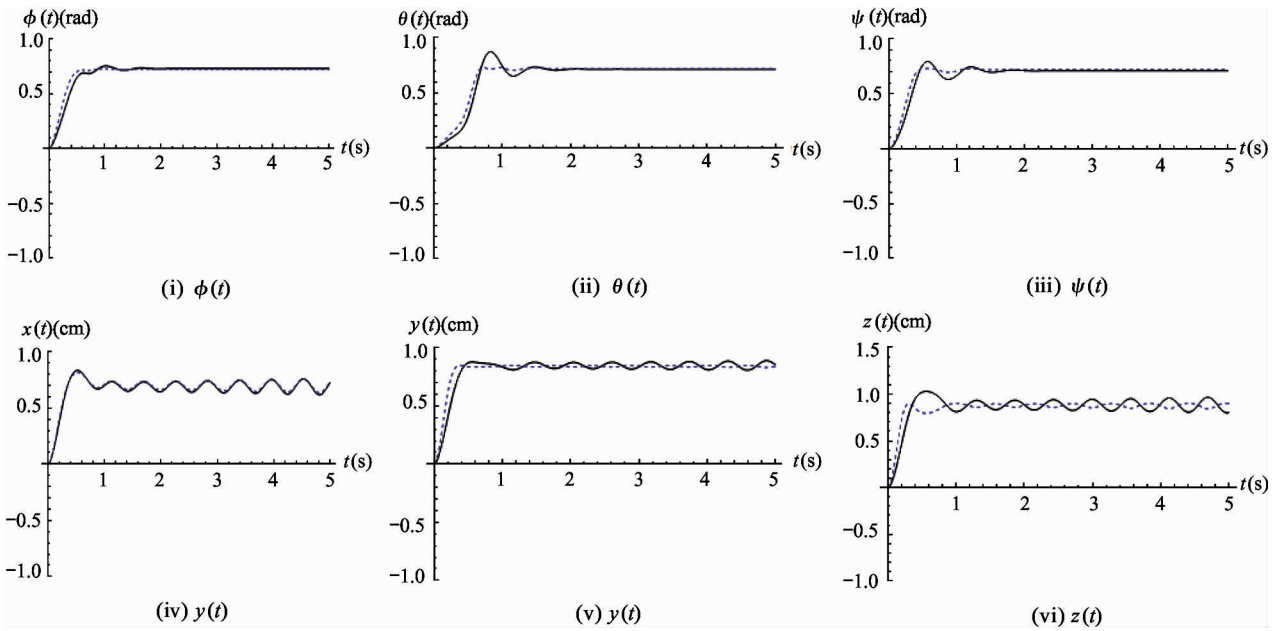

Fig. 10 The curve of attitude at hovering state

The initial angular displacement is changed into 10^{-1} rad with the same initial angular velocities p, q and r are equivalent to 0. The results of the attractor are not changed significantly, which demonstrates that the system is not sensitive to the initial condition. This result denotes the system is stable, as shown in Fig. 12 (i), (ii) and (iii).

3 Experimental results

The ducted fan UAV's flight experience is used to Pixhawk's flight control development environment, as shown in Fig. 13. When the value of rotor radius r is equivalent to 0.6 m, the dynamics stability of the vehicle is much better than that of r which is equivalent to 0.4 m in the case of the landing state.

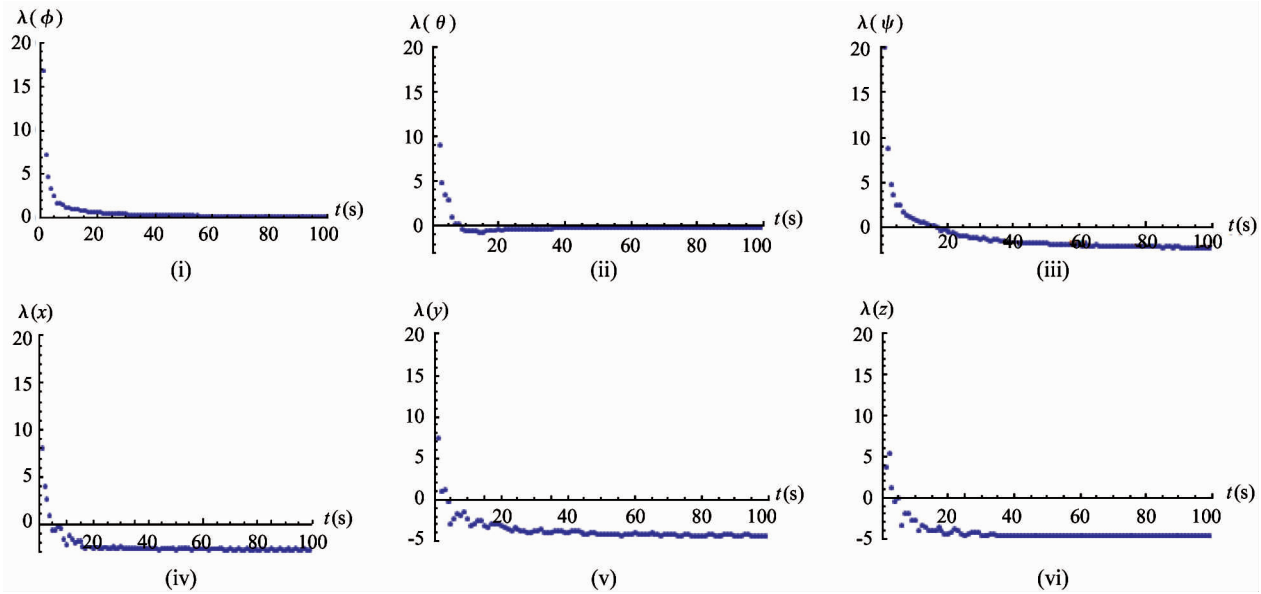

Fig. 11 Lyapunov exponents spectrum at hovering state

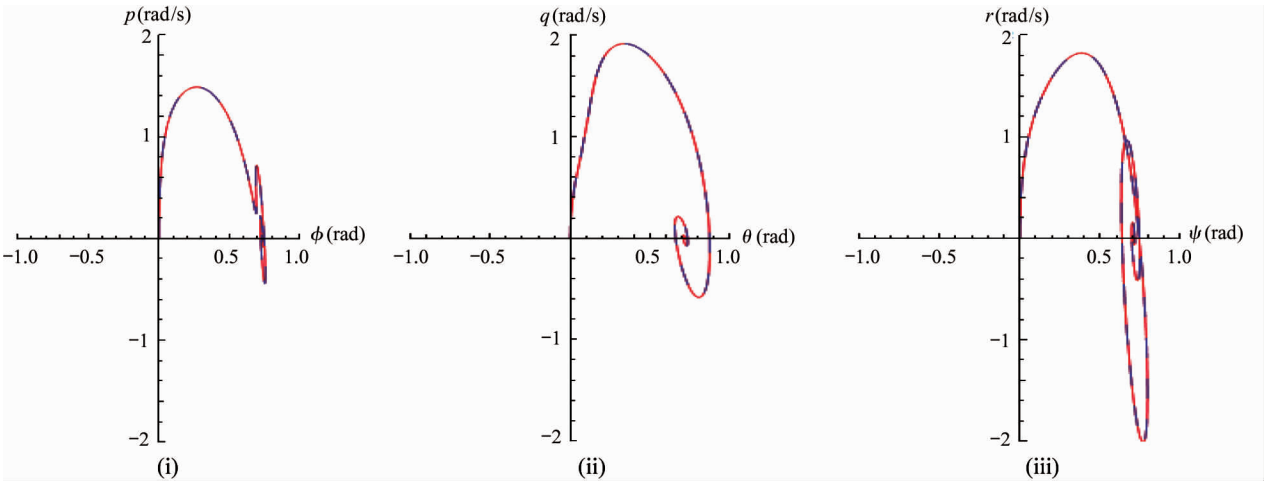

Fig. 12 Attractor of the state space

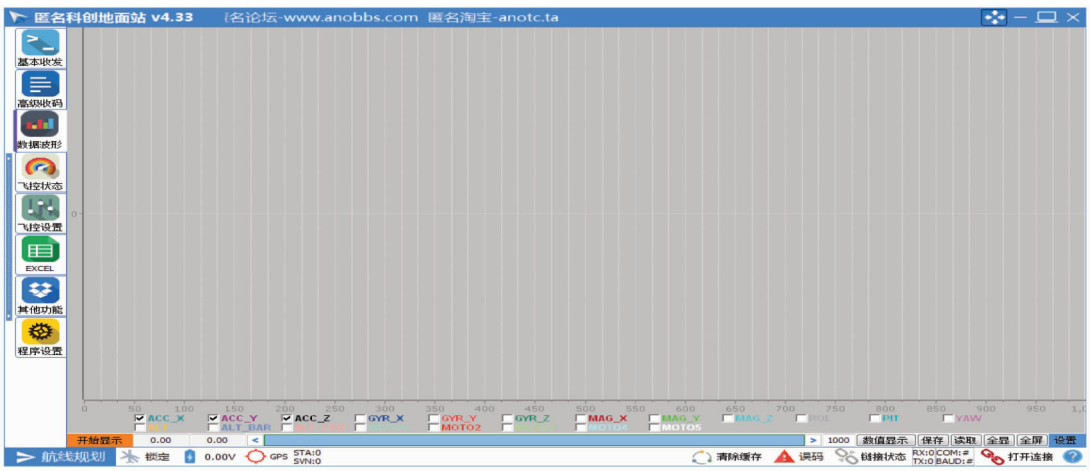

Fig. 13 Online interface of the Pixhawk's flight control development environment

Seeing from Figs14, 15 and 16, which are derived from the online interface of the Pixhawk's flight control development environment, and Figs14, 15 and 16 are linear displacement parameters in x, y and z axes, respectively. It can be easily shown that the attitude angle of the ducted fan UAVs has much better convergence to 0 in the value of rotor radius r equivalent to 0.6 m than that of r equivalent to 0.4 m according to Figs17, 18 and 19 in landing stage. This conclusion can be used to verify the results of comparison of Fig. 6 with 8. In summary, the optimization of mechanical-structure parameters can be used to improve the dynamics stability.

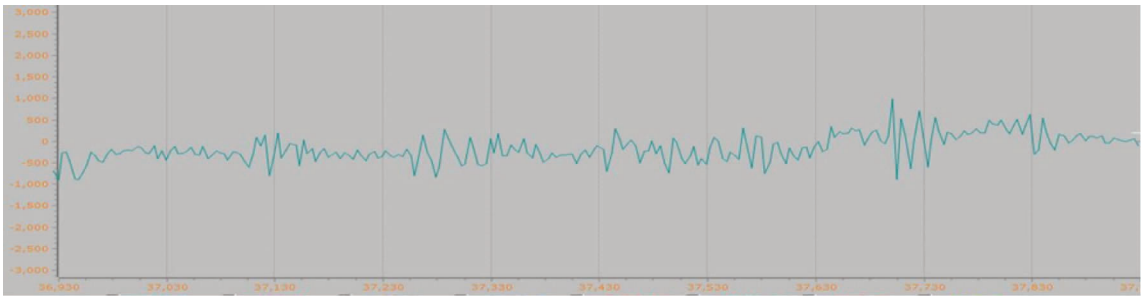

(i) $r=0.4$ m

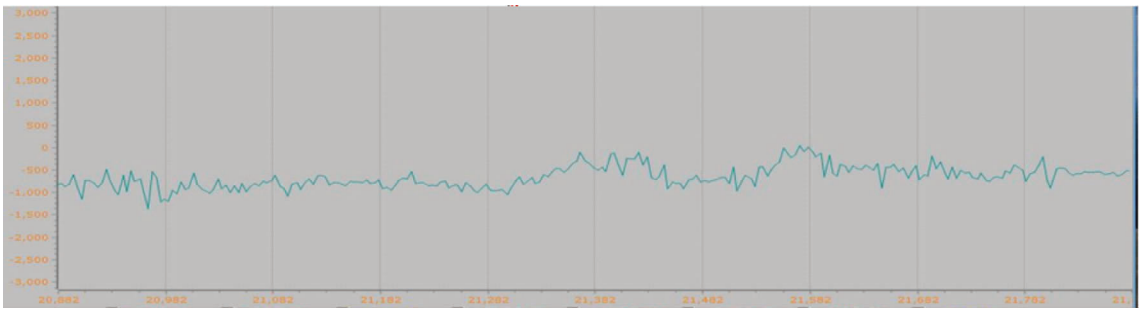

(ii) $r=0.6$ m

Fig. 14 Experimental attitude of the curve location parameter of in the x axis during landing state

(i) $r=0.4$ m

(ii) $r=0.6$ m

Fig. 15 Experimental attitude of the curve location parameter of in the y axis during landing state

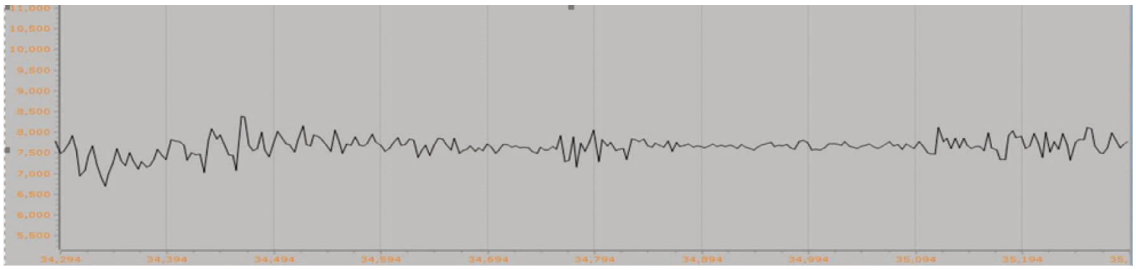

(i) $r = 0.4$ m

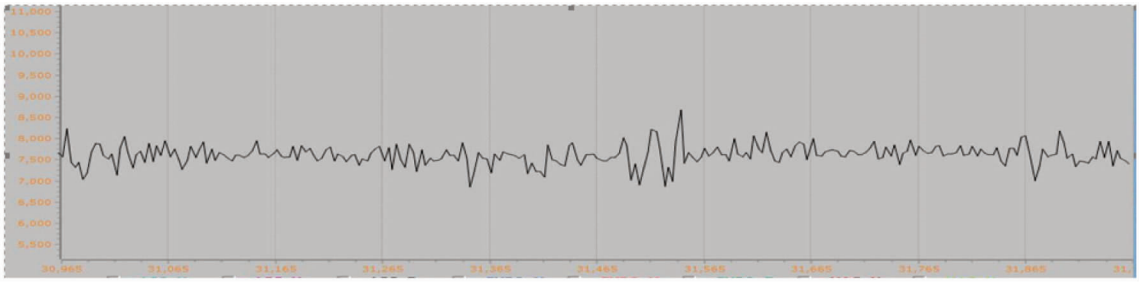

(ii) $r = 0.6$ m

Fig. 16 Experimental attitude of the curve location parameter of in the z axis during landing state

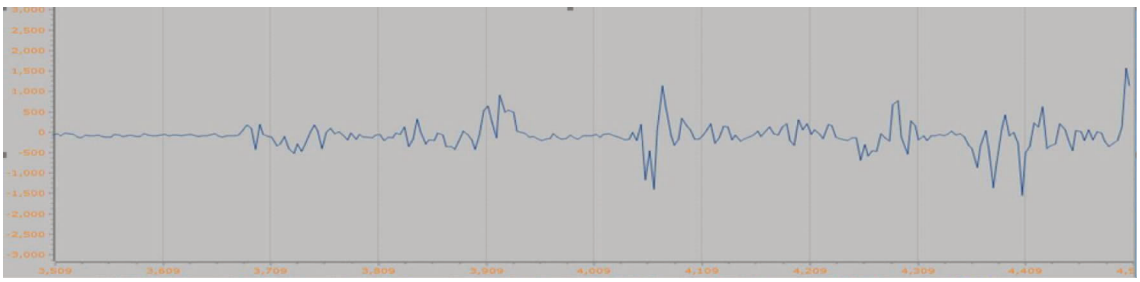

(i) $r = 0.4$ m

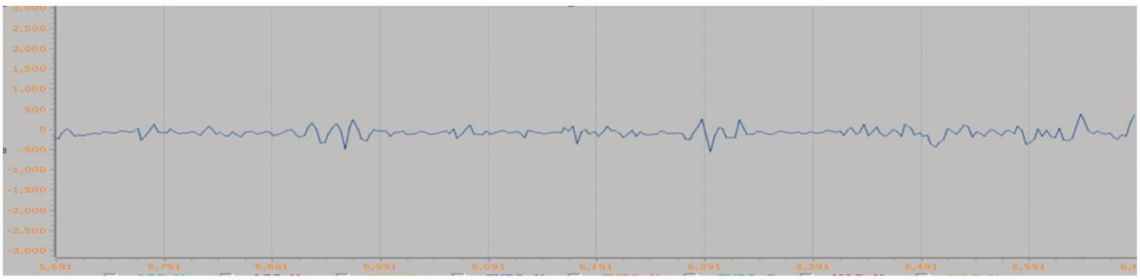

(ii) $r = 0.6$ m

Fig. 17 Experimental attitude of the curve angular in the x axis during landing state

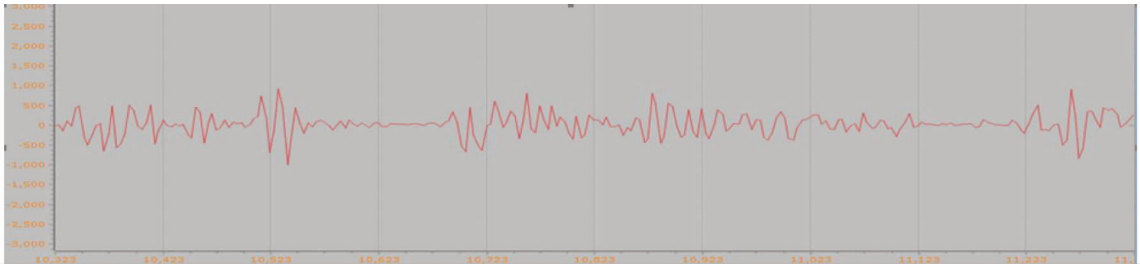

(i) $r = 0.4$ m

Fig. 18 Experimental attitude of the curve angular in the y axis during landing state

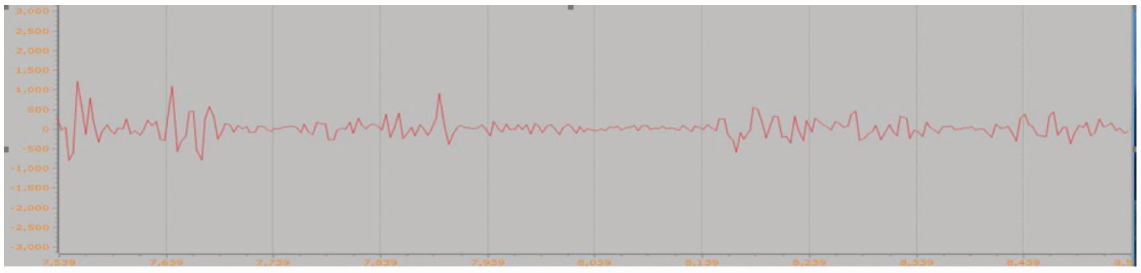

(ii) $r=0.6$ m

Fig. 18 Experimental attitude of the curve angular in the y axis during landing state

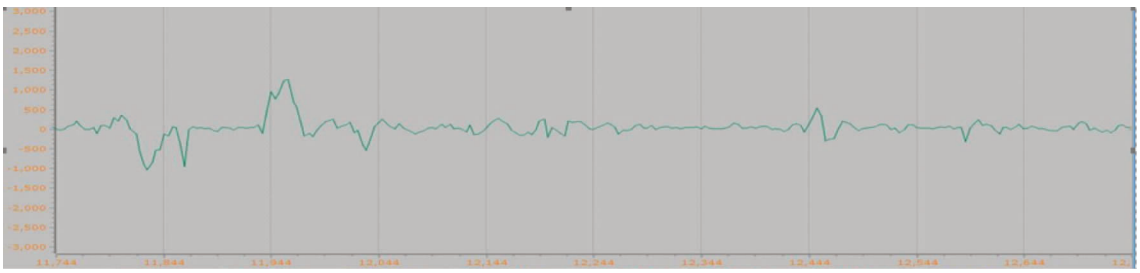

(i) $r=0.4$ m

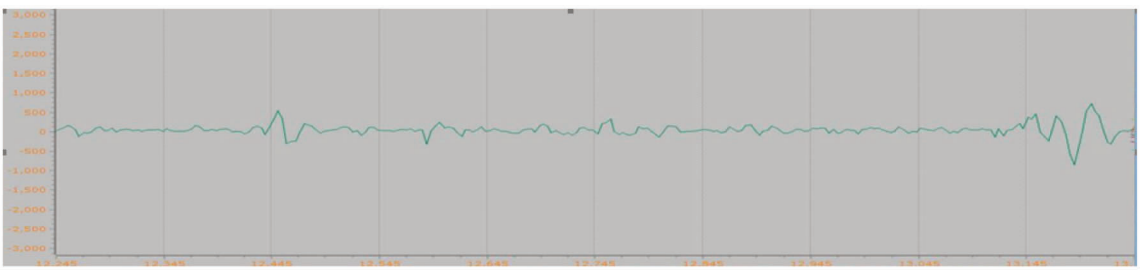

(ii) $r=0.6$ m

Fig. 19 Experimental attitude of the curve angular in z axis at landing state

4 Conclusions

The dynamic stability analysis is very important for the progress of the ducted fan UAVs. This article uses the concept of LEs to establish the quantification relationship between the ducted fan UAV's mechanical-structure parameters and its motion stability by optimizing mechanical-structure parameters to increase dynamics stability.

Three different stages of stability, such as take off, landing and hovering stage, respectively, have been analyzed in this article using the concept of LEs for the ducted fan UAVs. In the case of landing stage stability analysis, the radius ranges of a rotor where the vehicle stability is guaranteed have been changed. It is shown the significant insights into the effects of mechanical-structure parameters on dynamics stability. Moreover, the state space is another important property of a dynamics system. To investigate the effect of the initial condition on state space, the proportional-derivative (PD) controller has been presented for the hovering state. The disturbance of system stability comes from initial conditions. It can be derived that the vehicle is stable and will return to its stable fixed point, which verifies the stability under the suitable proportional and derivative controller. The conclusion is that the optimization of mechanical-structure parameters has exerted significant effects on its stability.

References

[1] Wang S H. Robust model for the design of controller in saucer UAV [J]. *Journal of Software*, 2010, 5(7): 753-760

[2] Amiri N, Ramirez-Serrano A, Davies R J. Integral back stepping control of an unconventional dual-Fan unmanned aerial vehicle [J]. *Journal Intelligent Robot System*, 2013, 69(1-4): 147-159

[3] Corsini A, Rispoli F, Sheard A G. Computational analysis of noise reduction devices in axial fans with stabilized finite element formulations [J]. *Computational Mechanics*, 2012, 50(6): 695-705

[4] Wang Z J, Chen L, Guo S J. Numerical analysis of aerodynamic characteristics for the design of a small ducted

fan aircraft [J]. *Journal of Aerospace Engineering*, 2012, 227 (10): 1556-1570
[5] Shin J. Indoor hovering control of small ducted-fan type OAV using ultrasonic positioning system[J]. *Journal of Intelligent Robot System*, 2011, 61(1-4): 15-27
[6] Liu Y P, Li X Y, Wang T M. Quantitative stability of quadrotor unmanned aerial vehicles[J]. *Nonlinear Dynamic*, 2017, 87:1819-1833
[7] Tylikowski A. Dynamic stability of weak equations of continuous systems[J]. *Archive of Applied Mechanics*, 2009, 79(6-7): 659-665
[8] Liu Y P, Chen C, Wu H T, et al. Structural stability analysis and optimization of the quadrotor unmanned serial vehicle via the concept of Lyapunov exponents[J]. *International Journal of Advanced Manufacture Technology*, 2016, 85(5-8): 1-11
[9] Sekhavat P, Sepehri N, Wu Q. Calculation of Lyapunov exponents using nonstandard finite difference discretization scheme: a case study[J]. *Journal of Difference Equations and Applications*, 2004, 10 (4): 369-378
[10] Sadri S, Wu Q. Stability analysis of a nonlinear vehicle model in plane motion using the concept of Lyapunov exponents[J]. *Vehicle of System Dynamic*, 2013, 51(6): 906-924
[11] Yang C X, Wu Q. On stability analysis via Lyapunov exponents calculated from a time series using nonlinear mapping a case study[J]. *Nonlinear Dynamic*, 2010, 59: 239-257
[12] Sun Y M, Wu Q. Stability analysis via the concept of Lyapunov exponents: a case study in optimal controlled biped standing[J]. *International Journal of Control*, 2012, 85 (12): 1952-1966
[13] Omar N, Ghada B, Abderrazak O. Global stabilization of an adaptive observer-based controller design applied to induction machine[J]. *International Journal of Advanced Manufacture Technology*, 2015, 81(1-4):423-432
[14] Amy M C, Richard J B. Structural analysis and optimization of tall buildings connected with sky bridges and atria [J]. *Structural and Multidisciplinary Optimization*, 2017, 55(2):583-600
[15] Polajnar M, Kosel F, Drazumeric R. Structural optimization using global stress-deviation objective function via the level-set method[J]. *Structural and Multidisciplinary Optimization*, 2017, 55(1): 91-104
[16] Salluce D N. Comprehensive System Identification of Ducted fan UAV. San Luis Obispo: California Polytechnic State University, 2004. 17-52
[17] Liu Y P, Huang X J, Wang T M, et al. Nonlinear dynamics modeling and simulation of two-wheeled self-balancing vehicle[J]. *International Journal of Advanced Robot System*, 2016, 13(6): 1-9
[18] Johnson E N, Turbe M A. Modeling, control, and flight testing of a small ducted fan aircraft[J]. *Journal of Guidance Control and Dynamics*, 2006, 29(4): 769-779
[19] Wang C H, Li Y W, Xi B Q, et al. Modeling, control and flight testing for a saucer ducted fan UAV[C]. In: Proceedings of the 3rd International Symposium on 2010 Systems and Control in Aeronautics and Astronautics (ISSCAA), Harbin, China, 2010. 930-935
[20] Martini A, Léonard F, Abba G. Dynamic modelling and stability analysis of model-scale helicopters under wind gust[J]. *International Journal of Advanced Robot System*, 2009, 54(4): 647-686
[21] Liu Y P, Li X Y, Wang T M, et al. Research on improvement of the dynamic stability of quadrotor unmanned aerial vehicles during take-off and landing[J]. *Chinese High Technology Letters*, 2015, 25(10-11): 927-934 (In Chinese)

Fu Weijie, born in 1969. He received his M. S. degree in School of Instrument Science & Engineering of Southeast University in 1999. He also received his B. S. degree from Xi'an Jiaotong University in 1991. His research interests include the intelligent robots.